The Journal of Chemical Physics

# Calculation of the residual entropy of Ice Ih by Monte Carlo simulation with the combination of the replica-exchange Wang–Landau algorithm and multicanonical replica-exchange method

Cite as: J. Chem. Phys. **154**, 044503 (2021); https://doi.org/10.1063/5.0038157
Submitted: 20 November 2020 • Accepted: 28 December 2020 • Published Online: 25 January 2021

Takuya Hayashi, Chizuru Muguruma and Yuko Okamoto

The Journal of Chemical Physics ARTICLE scitation.org/journal/jcp

# Calculation of the residual entropy of Ice Ih by Monte Carlo simulation with the combination of the replica-exchange Wang–Landau algorithm and multicanonical replica-exchange method

Cite as: J. Chem. Phys. 154, 044503 (2021); doi: 10.1063/5.0038157
Submitted: 20 November 2020 • Accepted: 28 December 2020 •
Published Online: 25 January 2021



Takuya Hayashi,[1,a)] Chizuru Muguruma,[2,b)] and Yuko Okamoto[1,3,4,c)]

## AFFILIATIONS

[1]Department of Physics, Graduate School of Science, Nagoya University, Nagoya, Aichi 464-8602, Japan
[2]Faculty of Liberal Arts and Sciences, Chukyo University, Toyota, Aichi 470-0393, Japan
[3]Center for Computational Science, Graduate School of Engineering, Nagoya University, Nagoya, Aichi 464-8603, Japan
[4]Information Technology Center, Nagoya University, Nagoya, Aichi 464-8601, Japan

[a)]**Electronic mail:** tahayashi@tb.phys.nagoya-u.ac.jp
[b)]**Electronic mail:** muguruma@lets.chukyo-u.ac.jp
[c)]**Author to whom correspondence should be addressed:** okamoto@tb.phys.nagoya-u.ac.jp

## ABSTRACT

We estimated the residual entropy of Ice Ih by the recently developed simulation protocol, namely, the combination of the replica-exchange Wang–Landau algorithm and multicanonical replica-exchange method. We employed a model with the nearest neighbor interactions on the three-dimensional hexagonal lattice, which satisfied the ice rules in the ground state. The results showed that our estimate of the residual entropy is in accordance with various previous results. In this article, we not only give our latest estimate of the residual entropy of Ice Ih but also discuss the importance of the uniformity of a random number generator in Monte Carlo simulations.



## I. INTRODUCTION

After the experimental discovery that the Ice Ih has non-zero residual entropy near zero temperature,[1] the theoretical explanation about the origin was proposed by the ice rules,[2,3] which considered the hydrogen bonds between water molecules in ice. The residual entropy per water molecule $S_0$ is proportional to the logarithm of the number of degrees of freedom of the orientations of one water molecule $W_0$,

$$S_0 = k_B \ln W_0. \tag{1}$$

Here, $k_B$ is the Boltzmann constant. The estimate by Pauling was $W_0^{\text{Pauling}} = 1.5$ and $S_0^{\text{Pauling}} = R \ln W_0^{\text{Pauling}} \simeq 0.806$ [cal/(mol K)].[3] Here, we have used $R = 8.314\,462\,618\ldots$ [J/(mol K)] for the gas constant on the NIST website[4] and the relation 1[cal] = 4.184[J] ($R = 1.9872$[cal/(mol K)]). It was in accordance with the experimental value $S_0^{\text{Experiment}} = 0.82(5)$ [cal/(mol K)].[1] Error bars in this article are given with respect to the last digits in parentheses. However, it was shown that Pauling's estimate was a lower bound by Onsager and Dupuis[5] and the advanced theoretical approximation was obtained by Nagle.[6]

As for computational simulations, two simulation models (two-state model and the six-state model), which satisfied the ice rules in the ground state, were proposed and the value was estimated[7–10] by the *Multicanonical* (MUCA) *Monte Carlo* (MC) *method*[11,12] (for reviews, see Refs. 13 and 14). After these simulation models were

suggested, many research groups estimated the residual entropy by various computational approaches for the last decade (see Refs. 15–19). The estimates by computer simulations seem to be equal to or more accurate than the theoretical estimate by Nagle. Although the residual entropy of ice is becoming one of the good examples to test the accuracy of simulation algorithms, there seem to be small disagreements among the estimates. The exact residual entropy of Ice Ih has yet to be obtained.

In this article, we present our latest estimate of the residual entropy by the recently proposed MC simulation with the combination of the *Replica-Exchange Wang–Landau* (REWL) *algorithm*[20,21] and *Multicanonical Replica-Exchange Method* (MUCAREM),[22–24] which we refer to as REWL-MUCAREM.[25] REWL-MUCAREM can give us highly precise estimates of the density of states (DOS) and the entropy under appropriate computational conditions. We employed the two-state model.[7] Our latest result is in good agreement with the estimates by several research groups that used other simulation methods. In addition, we also report that the uniformity of the random numbers is important for MC simulations.

This article is organized as follows: In Sec. II, we summarize the results of previous research studies briefly, and we explain the ice model that we employed and the REWL-MUCAREM protocol. In Sec. III, the simulation details are given. In Sec. IV, our results are presented and the importance of random numbers is discussed, and Sec. V is devoted to conclusions.

## II. METHODS

### A. Residual entropy

Figure 1 shows the hexagonal crystal structure of Ice Ih in two-dimensional projections. Figures 1(a) and 1(b) correspond to the projection to the *xy*-plane and the *yz*-plane, respectively. We assume that the water molecules exist as $H_2O$ molecules in ice and hydrogen atoms can occupy one of the two places on each bond according to the ice rules in Refs. 2 and 3: (1) there is one hydrogen atom on each bond and (2) there are two hydrogen atoms near each oxygen atom.

Suppose that there are $N$ water molecules. The number of hydrogen atoms is $2N$. The theoretical residual entropy $S_0$ per water molecule is defined by

$$S_0 = \frac{k_B \ln W}{N} = k_B \ln W_0, \tag{2}$$

where

$$W = (W_0)^N. \tag{3}$$

Here, $W$ is the total number of configurations of water molecules that satisfies the two ice rules. By defining $W_0$ as the number of orientations per water molecule, Pauling estimated the value to be[3]

$$W_0^{\text{Pauling}} = 1.5. \tag{4}$$

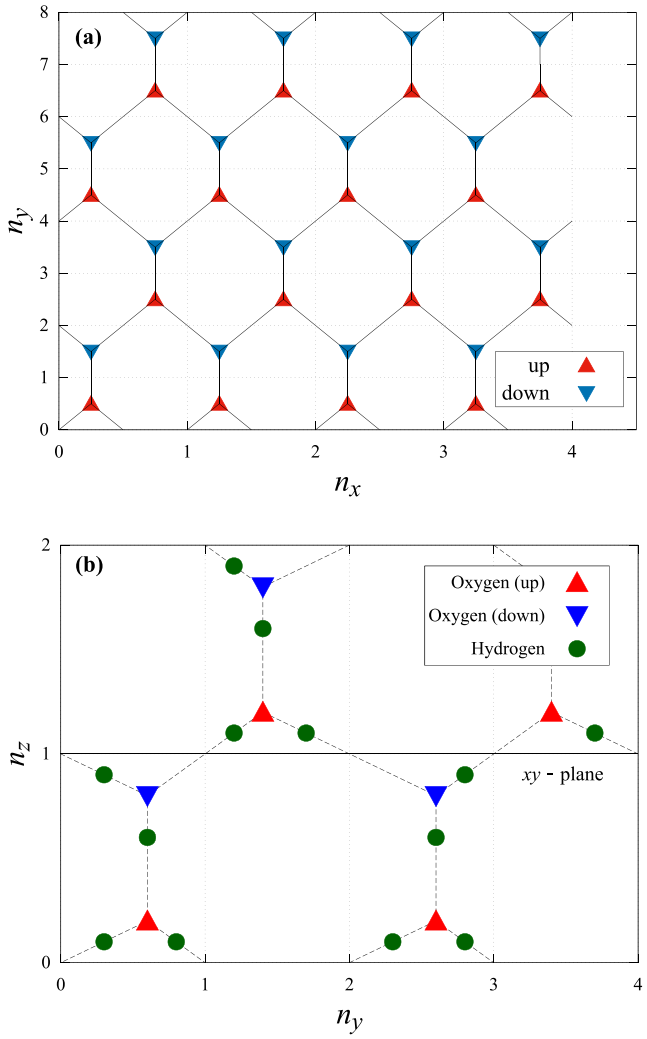


**FIG. 1.** Two-dimensional projection of Ice Ih. (a) Projection to the *xy*-plane and (b) projection to the *yz*-plane. The scale is different from the actual Ice Ih structure for simplicity. $n_x$, $n_y$, and $n_z$ are the numbers of sites along the *x*, *y*, and *z* axes, respectively. The total number of water molecules $N$ is given by $n_x \times n_y \times n_z$. The red triangles imply that the lattice points exist above the *xy*-plane, and the blue triangles imply that the lattice points exist below the *xy*-plane in (a). Oxygen atoms are located on lattice points. The triangles in (b) also represent the oxygen atoms. The dotted lines represent the hydrogen bonds pair of oxygen atoms. The filled green circles are hydrogen atoms on chemical bonds. Hydrogen atoms can occupy one of the two places on each bond according to the ice rules.

His strategy is as follows: ignoring the second ice rule (two hydrogen atoms exist near each oxygen atom), $2^{2N}$ configurations can be considered because each hydrogen atom is given the choice of two positions on each bond. There are 16 arrangements of the four hydrogen atoms around one oxygen atom, and only six arrangements can satisfy the second ice rule. Thus, the total number of configurations $W$ that satisfies the ice rule (1) and ice rule (2) simultaneously is

$$W = (W_0^{\text{Pauling}})^N = 2^{2N} \times \left(\frac{6}{16}\right)^N = \left(\frac{3}{2}\right)^N. \tag{5}$$

Equation (5) can be converted to the residual entropy as

$$S_0^{\text{Pauling}} = k_B \ln\left(W_0^{\text{Pauling}}\right) = 0.805\,74\cdots\,[\text{cal}/(\text{mol K})]. \tag{6}$$

Onsager and Dupuis showed that $W_0^{\text{Pauling}} = 1.5$ is in fact a lower bound because Pauling's arguments omitted the effects of closed loops.[5] Nagle used a series expansion method in order to refine the theoretical estimate.[6] The contribution coming from short closed loops was taken into account counting the graphs of the loops directly, and the effects of long loops were estimated by extrapolation based on the results of short loops. The approximate value was

$$W_0^{\text{Nagle}} = 1.506\,85(15), \tag{7}$$

and

$$S_0^{\text{Nagle}} = 0.814\,80(20)\cdots\,[\text{cal}/(\text{mol K})]. \tag{8}$$

Here, the error bar is not statistical but reflects higher-order corrections of the expansion, which are not entirely under control. In terms of theoretical approximation, another series expansion method, which used numerical linked cluster (NLC) expansion, was proposed.[26]

With the development of computer science, many research groups have tried to estimate the residual entropy by various computational approaches [for example, the thermodynamic integration method, Wang–Landau algorithm, and projected entangled-pair states (PEPS) algorithm].[15–19] However, there remain small differences between these results. Here, we give our latest estimate by the REWL-MUCAREM protocol in this article.

### B. Models

We used the two-state model.[7] In this model, we do not consider distinct orientations of the water molecules [the ice rule (2) is ignored] but allow two positions for each hydrogen nucleus between two oxygen atoms [the ice rule (1) is always satisfied]. The total potential energy $E$ of this system is given by

$$E = -\sum_i f\left(i, b_i^1, b_i^2, b_i^3, b_i^4\right), \tag{9}$$

where $i$ stands for the site number of oxygen atoms. The sum is over all sites (oxygen atoms) of the lattice. The function $f$ is defined by

$$f\left(i, b_i^1, b_i^2, b_i^3, b_i^4\right) = \begin{cases} 2 & \text{for two hydrogen nuclei close to } i \\ 1 & \text{for one or three hydrogen nuclei close to } i \\ 0 & \text{for zero or four hydrogen nuclei close to } i. \end{cases} \tag{10}$$

The ground state of this model fulfills the two ice rules completely. The energy at the ground state $E_{\text{ground}}$ is $-2N$. Because the normalization [the total number of configurations $\sum_E n(E)$ is $2^{2N}$, where $n(E)$ is the number of states at energy $E$] is known, MUCA simulations allow us to estimate the number of the configurations at the ground state accurately by calculating the ratio of $\tilde{n}(E_{\text{ground}})$ to $\sum_E \tilde{n}(E)$,[27] namely, we have

$$W = (W_0)^N = n(E_{\text{ground}}) = 2^{2N} \times \frac{\tilde{n}(E_{\text{ground}})}{\sum_E \tilde{n}(E)}. \tag{11}$$

Here, $\tilde{n}(E)$ is the unnormalized number of states obtained from MUCA simulations.

### C. Computational methods

We used an advanced generalized-ensemble MC algorithm that we recently developed, REWL-MUCAREM.[25] In this protocol, the DOS (i.e., the inverse of the multicanonical weight factor) is first determined roughly by a REWL simulation and then the DOS is refined by repeating MUCAREM simulations.

A brief explanation of MUCA[11–14] is now given here. The multicanonical probability distribution of potential energy $P_{\text{MUCA}}(E)$ is defined by

$$P_{\text{MUCA}}(E) \propto g(E) W_{\text{MUCA}}(E) \equiv \text{const}, \tag{12}$$

where $W_{\text{MUCA}}(E)$ is the multicanonical weight factor, the function $g(E)$ is the DOS, and $E$ is the total potential energy. By omitting a constant normalization factor, we have

$$W_{\text{MUCA}}(E) = \frac{1}{g(E)}. \tag{13}$$

In MUCA MC simulations, the trial moves are accepted with the following Metropolis transition probability $w(E \to E')$:

$$w(E \to E') = \min\left[1, \frac{W_{\text{MUCA}}(E')}{W_{\text{MUCA}}(E)}\right] = \min\left[1, \frac{g(E)}{g(E')}\right]. \tag{14}$$

Here, $E$ is the potential energy of the original configuration and $E'$ is that of a proposed one. After a long production run, the best estimate of the DOS can be obtained by the single-histogram reweighting techniques,[28]

$$g(E) = \frac{H(E)}{W_{\text{MUCA}}(E)}, \tag{15}$$

where $H(E)$ is the histogram of sampled potential energy. Practically, the $W_{\text{MUCA}}(E)$ is set to $\exp[-\beta E]$ at first and modified by repeating sampling and reweighting. Here, $\beta$ is the inverse of temperature $T$ ($\beta = 1/k_B T$).

The *Wang–Landau* (WL) algorithm[29,30] also uses $1/g(E)$ as the weight factor, and the Metropolis criterion is the same as in Eq. (14). However, $g(E)$ is updated dynamically as $g(E) \to f \times g(E)$ during the simulation when the simulation visits a certain energy value $E$, where $f$ is a modification factor. We continue the updating until the histogram $H(E)$ becomes flat. If $H(E)$ is flat enough, a next simulation begins after resetting the histogram to zero and reducing the modification factor (usually, $f \to \sqrt{f}$). The flatness evaluation can be done in various ways. This process is terminated when the modification factor attains a predetermined value $f_{\text{final}}$, and $\exp(10^{-8}) \simeq 1.000\,000\,01$ is often used as $f_{\text{final}}$. Hence, the estimated $g(E)$ tends to converge to the true DOS of the system within this much accuracy set by $f_{\text{final}}$.

MUCA can be combined with the *Replica-Exchange Method* (REM)[31–33] for more efficient sampling (REM is also referred to as *parallel tempering*.[34]). The method is referred to as MUCAREM.[22–24] In MUCAREM, the entire energy range of interest $[E_{\min}, E_{\max}]$ is divided into $M$ sub-regions, $E_{\min}^{\{m\}} \le E \le E_{\max}^{\{m\}}$ $(m = 1, 2, \ldots, M)$, where $E_{\min}^{\{1\}} = E_{\min}$ and $E_{\max}^{\{M\}} = E_{\max}$. There should be some overlaps between the adjacent regions. MUCAREM uses $M$ replicas of the original system. The weight factor for sub-region $m$ is defined by[22–24]

$$W_{\text{MUCA}}^{\{m\}}(E) = \begin{cases} e^{-\beta_{\text{L}}^{\{m\}} E} & \text{for } E < E_{\min}^{\{m\}} \\ \dfrac{1}{g_m(E)} & \text{for } E_{\min}^{\{m\}} \le E \le E_{\max}^{\{m\}} \\ e^{-\beta_{\text{H}}^{\{m\}} E} & \text{for } E > E_{\max}^{\{m\}}, \end{cases} \tag{16}$$

where $g_m(E)$ is the DOS for $E_{\min}^{\{m\}} \le E \le E_{\max}^{\{m\}}$ in sub-region $m$, $\beta_{\text{L}}^{\{m\}} = d\ln[g_m(E)]/dE$ $(E = E_{\min}^{\{m\}})$, and $\beta_{\text{H}}^{\{m\}} = d\ln[g_m(E)]/dE$ $(E = E_{\max}^{\{m\}})$. The MUCAREM weight factor $W_{\text{MUCAREM}}(E)$ for the entire energy range is expressed by the following formula:

$$W_{\text{MUCAREM}}(E) = \prod_{m=1}^{M} W_{\text{MUCA}}^{\{m\}}(E). \tag{17}$$

After a certain number of independent MC steps, replica exchange is proposed between two replicas, $i$ and $j$, in neighboring sub-regions, $m$ and $m+1$, respectively. The transition probability, $w_{\text{MUCAREM}}$, of this replica exchange is given by

$$w_{\text{MUCAREM}} = \min\left[1, \frac{W_{\text{MUCA}}^{\{m\}}(E_j) W_{\text{MUCA}}^{\{m+1\}}(E_i)}{W_{\text{MUCA}}^{\{m\}}(E_i) W_{\text{MUCA}}^{\{m+1\}}(E_j)}\right], \tag{18}$$

where $E_i$ and $E_j$ are the energies of replica $i$ and replica $j$ before the replica exchange, respectively. If replica exchange is accepted, the two replicas exchange their weight factors $W_{\text{MUCA}}^{\{m\}}(E)$ and $W_{\text{MUCA}}^{\{m+1\}}(E)$ and energy histograms $H_m(E)$ and $H_{m+1}(E)$. The final estimate of the DOS can be obtained from $H_m(E)$ after a long production simulation by the multiple-histogram reweighting techniques[35,36] or weighted histogram analysis method (WHAM).[36]

Let $n_m$ be the total number of samples for the $m$th energy sub-region. The final estimate of the DOS, $g(E)$, is obtained by solving the following WHAM equations self-consistently by iteration:[22–24]

$$\begin{cases} g(E) = \dfrac{\sum_{m=1}^{M} H_m(E)}{\sum_{m=1}^{M} n_m \exp(f_m) W_{\text{MUCA}}^{\{m\}}(E)}, \\ \exp(-f_m) = \sum_E g(E) W_{\text{MUCA}}^{\{m\}}(E). \end{cases} \tag{19}$$

Repeating these MUCAREM sampling and WHAM reweighting processes, we can obtain a more accurate DOS. Although the ordinary REM is often used to obtain the first estimate of the DOS in the MUCAREM iterations, we used the results of the REWL simulation[20,21] instead of the first REM run because REWL is stable and it can give a more accurate DOS.

The REWL method is essentially based on the same weight factors as in MUCAREM, while the WL simulations replace the MUCA simulations for each replica. This simulation is terminated when the modification factors on all sub-regions attain a certain minimum value $f_{\text{final}}$. After a REWL simulation, $M$ pieces of DOS fragments with overlapping energy intervals are obtained. The fragments need to be connected in order to determine the final DOS in the entire energy range $[E_{\min}, E_{\max}]$. The joining point for any two overlapping DOS pieces is chosen where the inverse microcanonical temperature $\beta(= \partial \ln[g(E)]/\partial E)$ coincides best.[20,21] This connecting process can be omitted in REWL-MUCAREM because the estimated DOS from WHAM is used directly as the multicanonical weight factor in MUCAREM. After repeating MUCAREM several times, the DOS with high accuracy is obtained. In this article, additional long MUCA production simulations were performed to obtain the final DOS with the highest accuracy and estimate the error. The MUCA weight factor for these production runs is determined from the obtained DOS after the REWL-MUCAREM simulations [see Eq. (13)].

## III. COMPUTATIONAL DETAILS

The total number of water molecules $N$ is given by $n_x \times n_y \times n_z$, where $n_x$, $n_y$, and $n_z$ are the numbers of sites along the $x$, $y$, and $z$ axis, respectively (see Fig. 1). The total number of sites (i.e., the total number of oxygen atoms) is $N$, and the total number of hydrogen atoms is $2N$. The values of $n_x$, $n_y$, and $n_z$ are restricted to $n_x = 1, 2, 3, \ldots$, $n_y = 4, 8, 12, \ldots$, and $n_z = 2, 4, 6, \ldots$ because we used periodic boundary conditions. The total number of molecules considered was $N = 128$, 288, 360, 576, 896, 1600, 2880, and 4704. The positions of hydrogen atoms were updated during MC simulations. Energy values were collected after each MC step. One MC sweep is defined as an evaluation of the Metropolis criterion $2N$ times.

The REWL-MUCAREM protocol was used in order to obtain the DOS. It corresponds to the number of configurations $n(E)$ at $E$. In MUCA and WL simulations, it is necessary to determine the entire energy range $[E_{\min}, E_{\max}]$ before starting simulations. We selected the values as follows: $[E_{\min}, E_{\max}] = [-2N, -5N/4]$. Here, $E_{\min}$ corresponds to the ground state and $E_{\max}$ corresponds

to the energy value around which the entropy takes the maximum value (see Fig. 2). Figure 2 shows the typical dimensionless entropy [ln $n(E)$] per water molecule in Ice Ih, which was obtained by our additional MUCA simulations for the system with $N = 2880$ under the condition $[E_{min}, E_{max}] = [-2N, 0]$. The dimensionless entropy takes the maximum value at $E/N = -5/4$. Thus, the inverse temperature $\beta$ takes the value 0 at $E_{max}$. Under the condition $[E_{min}, E_{max}] = [-2N, -5N/4]$, a flat MUCA probability distribution is realized in $-2N \le E \le -5N/4$ and a canonical probability distribution at $\beta = 0$ is obtained for $E > -5N/4$. The $n(E)$ was summed up to the maximum energy that was obtained during the simulations in order to estimate the total number of configurations. Although it is desirable to take $E_{max} = 0$ in order to estimate $W_0$ with high accuracy according to our normalization, it is sufficient that $E_{max}$ is $-5N/4$ because most of the configurations are distributed around $E = -5N/4$ and the number of configurations that takes much higher potential energy than $E = -5N/4$ can be neglected (see Fig. 3). Figure 3 shows the summation of $n(E)$ that was normalized at $E_{min}$ per water molecule for the system with $N = 128$. It was summed up from $E_{min}$ to $E$ ($E$ is a certain energy value). The summation is saturated at a little larger energy than $E/N = -5/4$. The difference between the asymptotic value and the value 16/6, which is the inverse value of Pauling's estimate 6/16 [compare Eqs. (5) and (11)], represents the effects of closed loops in Ref. 5. The inset in Fig. 3 shows the $n(E)$ directly. Most of the total number of configurations is distributed around the peak. These results imply that the sum of the number of states that takes much higher energy than $E/N = -5/4$ is sufficiently small not to have an effect on our estimates of the residual entropy. In fact, although we compared the estimate of $W_0$ under the condition $[-2N, -5N/4]$ with the estimate under the condition $[-2N, 0]$ up to the $N = 2880$ system, the difference was small enough within errors. As a result for $[E_{min}, E_{max}] = [-2N, -5N/4]$, we could obtain more samples at the ground state energy, which was most important for the estimation of the residual entropy during MUCA simulations.

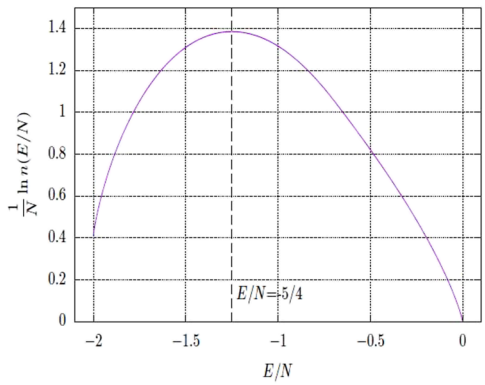


**FIG. 2**. Typical dimensionless entropy ln $n(E/N)$ per water molecule of Ice Ih as a function of potential energy per site ($E/N$). The values were obtained by an additional REWL-MUCAREM simulation for the $N = 2880$ system. ln $n(0)$ is set to ln(2) because the possible configures at $E = 0$ are two. The entropy takes the maximum value at the energy $E/N = -5/4$.

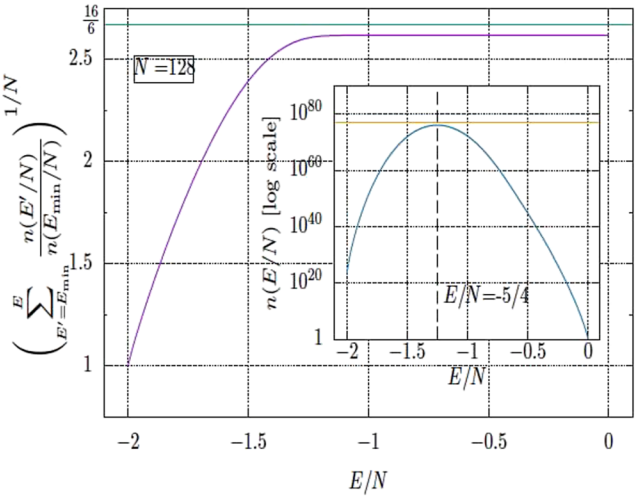


**FIG. 3**. The summation of $n(E/N)$ from $E_{min}$ to $E$ for system $N = 128$. The value is normalized at $E_{min}$ per water molecule. The horizontal green line shows the inverse of Pauling's estimate (6/16). The summation is saturated around a little larger potential energy than $E/N = -5/4$. The inset shows the $n(E/N)$ we obtained. Here, $n(0)$ is set to 2. The horizontal orange line shows the total number of configurations ($\sum_E n(E/N) = 2^{2N}$). $n(E/N)$ takes the maximum value at $E/N = -5/4$, and most of the total number of conformations is distributed around the peak.

In the REWL and MUCAREM simulations, 4–32 replicas were used depending on the number of water molecules. Each replica performed a WL simulation in REWL and a MUCA simulation in MUCAREM within their energy sub-regions, which had an overlap of about 80% between neighboring sub-regions. The replica exchange criterion and WL flatness criterion were tested during the simulations. The intervals for replica exchange and flatness tests depend on the lattice sizes (see Table I). In the WL flatness criterion of each replica, a flatness of $H_{min}/H_{max} > 0.5$ was considered sufficient for stopping the recursion and restarting a next WL iteration after resetting the recursion factor by $f \to \sqrt{f}$. Here, $H_{min}$ is the smallest value and $H_{max}$ is the largest value of the histogram $H(E)$. We iterated the $f$ reducing process 20 times, and we set $f_{final} \simeq 1.907\,35 \times 10^{-6}$. Once a rough estimate of the DOS was obtained by REWL, MUCAREM samplings and WHAM reweighting processes were then iterated five times in order to get a more precise DOS. The total number of MC sweeps for each MUCAREM was $2.0 \times 10^7$ sweeps.

After we obtained a DOS by REWL-MUCAREM, MUCA production runs with the MUCA weight factor determined by the obtained DOS were performed $M = 32$ times independently for evaluating the residual entropy and errors. Average values and errors were obtained by the following standard formulas:

$$\overline{n(E_{min})} = \frac{\sum_{i=1}^{M} n(E_{min})^{\{i\}}}{M}, \qquad \varepsilon_n = \sqrt{\frac{\sum_{i=1}^{M}\left(n(E_{min})^{\{i\}} - \overline{n(E_{min})}\right)^2}{M(M-1)}}. \tag{20}$$

**TABLE I**. Initial conditions in REWL-MUCAREM simulations.

| $N$ | $n_x$ | $n_y$ | $n_z$ | No. of replicas | Replica exchange[a] | WL criteria[b] | Total MC sweeps for REWL[c] | Total MC sweeps for MUCAREM[d] |
|---|---|---|---|---|---|---|---|---|
| 128 | 4 | 8 | 4 | 4 | 250 | 500 | $8.150 \times 10^4$ | $2.0 \times 10^7 \times 5$ |
| 288 | 4 | 12 | 6 | 8 | 250 | 500 | $2.795 \times 10^5$ | $2.0 \times 10^7 \times 5$ |
| 360 | 5 | 12 | 6 | 8 | 250 | 500 | $2.850 \times 10^5$ | $2.0 \times 10^7 \times 5$ |
| 576 | 6 | 12 | 8 | 16 | 500 | 1 000 | $4.410 \times 10^5$ | $2.0 \times 10^7 \times 5$ |
| 896 | 7 | 16 | 8 | 16 | 500 | 1 000 | $1.334 \times 10^6$ | $2.0 \times 10^7 \times 5$ |
| 1600 | 8 | 20 | 10 | 32 | 2500 | 5 000 | $2.530 \times 10^6$ | $2.0 \times 10^7 \times 5$ |
| 2880 | 10 | 24 | 12 | 32 | 2500 | 5 000 | $5.110 \times 10^6$ | $2.0 \times 10^7 \times 5$ |
| 4704 | 12 | 28 | 14 | 32 | 5000 | 10 000 | $1.637 \times 10^7$ | $2.0 \times 10^7 \times 5$ |

[a]The interval of replica exchange trial (MC sweeps) in REWL and MUCAREM.
[b]The interval of WL criteria check (MC sweeps) in REWL.
[c]Total MC sweeps per replica that are required for all WL weight factors $f$ to converge to $f_{\text{final}}$ in REWL.
[d]Total MC sweeps per each replica in MUCAREM. MUCAREM simulations were iterated 5 times.

Here, $n(E_{\min})^{\{i\}}$ is a measured value from the $i$th MUCA production simulation ($i = 1, 2, \ldots, M$). The total number of MC sweeps for measurement was $6.4 \times 10^8$ sweeps for each MUCA production run. The single-histogram reweighting techniques in Eq. (15) were employed in order to obtain the final estimates for $W_0$ by Eq. (11).

Random number generators have a large effect on the MC method. In this article, the Mersenne Twister random number generator was employed.[37] We used the program code on an open source.[38]

## IV. RESULTS AND DISCUSSION

### A. Calculations of residual entropy

Figure 4 shows the time series of the energy-range index of one of the replicas (replica 1) during the final MUCAREM simulation for the $N = 4704$ system. Here, we used 32 replicas. The total energy range $[E_{\min}, E_{\max}]$ was divided into 32 sub-regions. $E_{\min}$ was $-9408$ and $E_{\max}$ was $-5880$. The minimum energy label was 1, and the maximum energy label was 32. It can be seen that replica 1 went from label 1 to label 32 and came back many times. This means that replica exchange worked properly. Figure 5 shows the time series of the potential energy of one of the replicas (replica 1) for the same simulation as in Fig. 4. The replica made a random walk in energy space. There is a strong correlation between the energy-range index in Fig. 4 and the potential energy in Fig. 5, as expected. The four figures in Fig. 6 show the histograms of potential energy that were obtained by the final MUCAREM simulation for the $N = 4704$ system. Each energy label corresponds to the sub-region $m$ ($m = 1, 2, 3, 4$). Although we used 32 sub-regions, the results for only the first four sub-regions are shown in Fig. 6. Each histogram shows a flat distribution.

Figure 7 shows the logarithm of our final DOS by the REWL-MUCAREM protocol for $N = 4704$, and Fig. 8 shows the energy histogram obtained after the MUCA production runs that used the

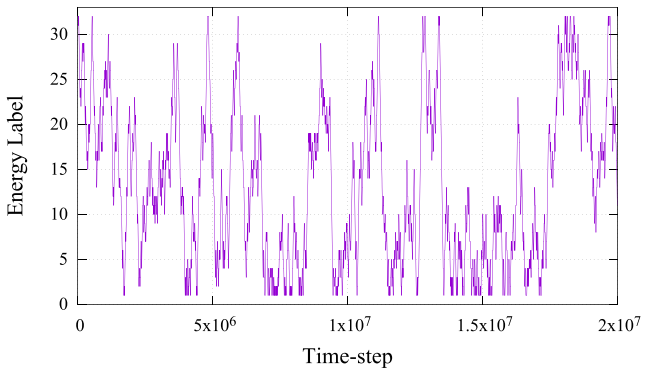


**FIG. 4**. History of the energy-range index (energy label) of one of the replicas (replica 1) during the final MUCAREM simulation for $N = 4704$.

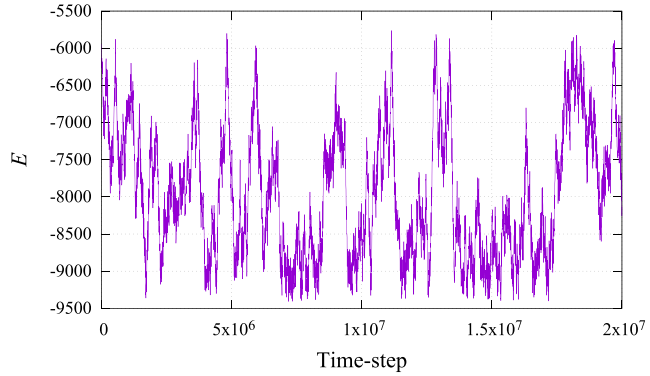


**FIG. 5**. History of the potential energy of one of the replicas (replica 1) during the final MUCAREM simulation for $N = 4704$.

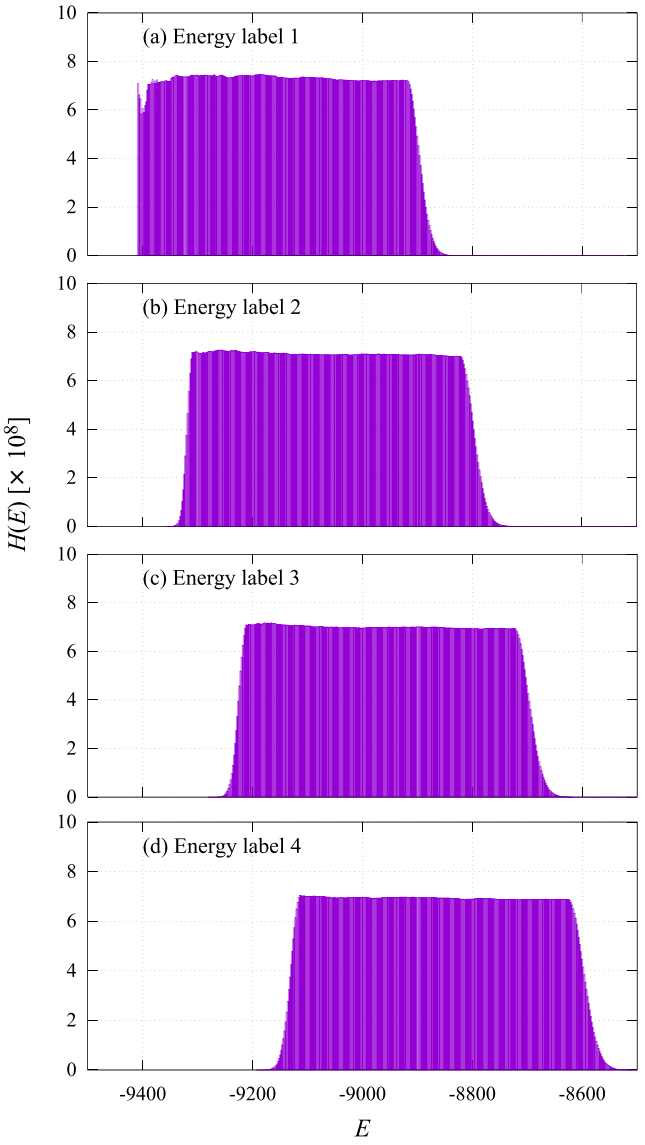


**FIG. 6**. Histograms of potential energy obtained by the final MUCAREM simulation of the water molecules $N = 4704$. Each energy label corresponds to the sub-region $m = 1, 2, 3, 4$. Sub-regions have an overlap of about 80% between neighboring sub-regions. Each histogram shows a flat distribution.

final DOS obtained from the final REWL-MUCAREM simulation as the weight factor [see Eq. (13)]. The ideal MUCA weight factor makes a completely flat histogram. The flatness values ($H_{\min}/H_{\max}$) after MUCA production runs are listed in Table II, and the values are larger than 0.8 in all systems. We remark that the flatness criterion for our WL simulations was 0.5. It means that our estimate of the DOS by the REWL-MUCAREM protocol is very accurate indeed. Similar results were obtained in all system sizes.

The tunneling events during the MUCA production runs were also counted. Here, a tunneling event is defined by a trajectory that

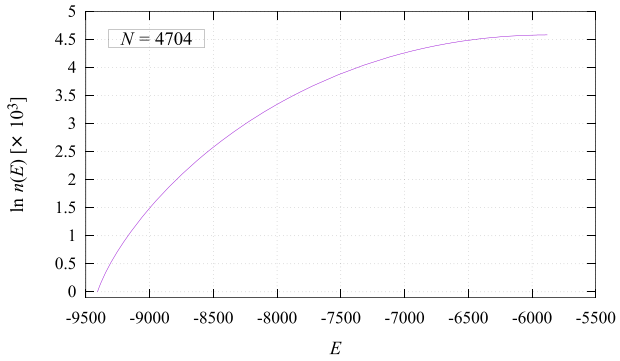


**FIG. 7**. The entropy as a function of energy $E$ estimated by the REWL-MUCAREM simulation for $N = 4704$. Here, the value of $\ln n(E)$ at $E = -9408$ is set equal to 0.

goes from $E_{\min}$ to $E_{\max}$ and back (or that goes from $E_{\max}$ to $E_{\min}$ and back). Table II lists the total number of tunneling events of 32 independent MUCA production runs. A lot of tunneling events were indeed observed in all system sizes. It implies that the observed configurations changed dramatically during the simulation many times. We conclude that our REWL-MUCAREM protocol and MUCA production run worked properly from these results.

Our estimates of $W_0$ are also listed in Table II. The values obtained from Eq. (20) and the extrapolation are shown in Fig. 9. We used the following form as an extrapolation formula:

$$W_0\left(\frac{1}{N}\right) = W_0(0) + a\left(\frac{1}{N}\right)^{\theta}. \tag{21}$$

Here, $\theta \neq 1$ reflects bond correlations in the ground state.[7] The final estimate of $W_0^{\text{This Work}}$ [which is equal to $W_0(0)$ in Fig. 9] is given in the second-to-last column in Table II. Although the data point for the smallest lattice size ($N = 128$) was included in the fitting in our previous works,[7,10] this data point was not included in the fitting in

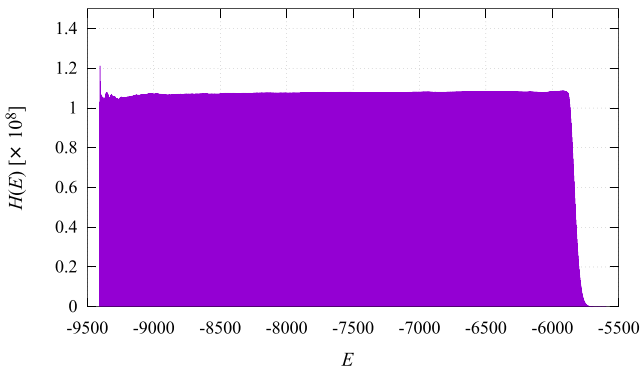


**FIG. 8**. Total histogram of potential energy obtained by the MUCA production simulation for $N = 4704$. The entropy in Fig. 7 was used as the MUCA weight factor.

**TABLE II**. Estimated residual entropy of Ice Ih.

| $N$ | $n_x$ | $n_y$ | $n_z$ | Tunneling[a] | Flatness[b] | $W_0$[c] | $S_0$[c] |
|---|---|---|---|---|---|---|---|
| 128 | 4 | 8 | 4 | 7 637 621 | 0.990 68 | 1.528 623 7(338) | 0.843 303 7(404) |
| 288 | 4 | 12 | 6 | 1 603 919 | 0.972 33 | 1.517 599 2(309) | 0.828 920 0(405) |
| 360 | 5 | 12 | 6 | 1 019 315 | 0.947 45 | 1.515 599 5(314) | 0.826 299 8(412) |
| 576 | 6 | 12 | 8 | 412 944 | 0.954 16 | 1.512 784 5(264) | 0.822 605 4(347) |
| 896 | 7 | 16 | 8 | 180 083 | 0.944 47 | 1.510 963 7(237) | 0.820 212 1(312) |
| 1600 | 8 | 20 | 10 | 57 543 | 0.938 00 | 1.509 517 6(236) | 0.818 309 3(311) |
| 2880 | 10 | 24 | 12 | 18 577 | 0.913 32 | 1.508 649 1(313) | 0.817 165 7(413) |
| 4704 | 12 | 28 | 14 | 6 591 | 0.830 09 | 1.508 202 9(360) | 0.816 577 9(475) |
| $\infty$ | | Fitting | | | | 1.507 472 3(474)[d] | 0.815 615 0(625)[d] |

[a]The total counts of observed tunneling events during 32 MUCA production runs.
[b]The value of flatness ($H_{max}/H_{min}$) calculated by accumulating the histograms after 32 MUCA production runs.
[c]The values in parentheses represent the errors obtained by 32 MUCA production runs and fitting using Eq. (20). The error bars for $S_0$ and $\Delta S_0$ were calculated by $\Delta S_0 = k_B \Delta W_0 / W_0$.
[d]The data point for the smallest lattice size ($N = 128$) was not included in the fitting in Eq. (21). The errors of each estimate of $W_0$ were considered in the fitting.

this article and in Fig. 9 because $N = 128$ is less than half of $N = 288$ and the results will be subject to large finite-size errors. In addition, we used the errors of $W_0(1/N)$ as weights for fitting.

The final estimate is

$$W_0(0) = 1.507\,472 \pm 0.000\,047. \tag{22}$$

This estimate converts into

$$S_0 = 0.815\,615 \pm 0.000\,063\ [\text{cal/(mol K)}]. \tag{23}$$

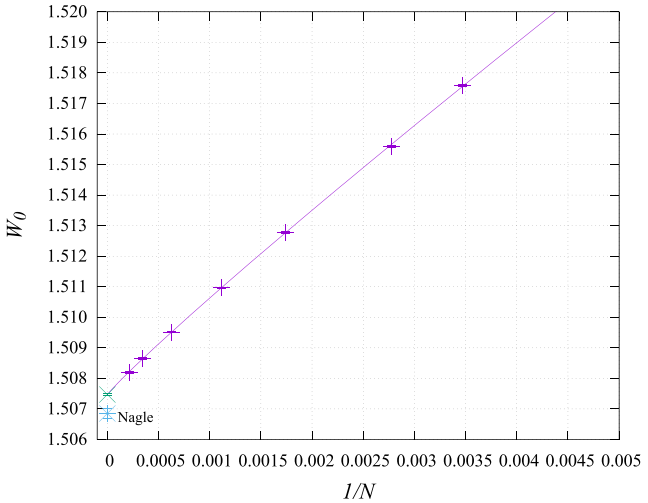


**FIG. 9**. The number of orientations of one water molecule $W_0(1/N)$ at the ground state as a function of the inverse of $N$. Error bars are smaller than the symbols.

The values of fitting parameters obtained by the MATHEMATICA were $a = 1.992\,074 \pm 0.119\,366$ and $\theta = 0.933\,296 \pm 0.011\,084$.

Some remarks are in order. Naturally, the final estimates in Eq. (22) will somewhat depend on the selection of data points that are included in the fitting, resulting in systematic errors. Our results were, for instance, $W_0(0) = 1.507\,401 \pm 0.000\,031$ with no points omitted, $1.507\,409 \pm 0.000\,057$ with the data for $N = 128$ and 288 omitted, and $1.507\,480 \pm 0.000\,078$ with the data for $N = 128$, 288, and 360 omitted. Note that in these three cases, the ranges of values within error bars overlap with those of the values in Eq. (22).

We want to compare our latest estimate of $W_0$ with the results of other research groups. In Fig. 10, the estimation values of $W_0$ with their error bars are plotted. Various calculation methods for $S_0$ and $W_0$ and their calculated values are summarized in Table III. The results of Berg,[7] Kolafa,[16] Ferreyra,[18] Vanderstraeten,[19] and the present work are consistent with each other within error bars. In particular, three different computational approaches (PEPS algorithm,[19] thermodynamic integration,[16] and REWL-MUCAREM) give almost the same estimates.

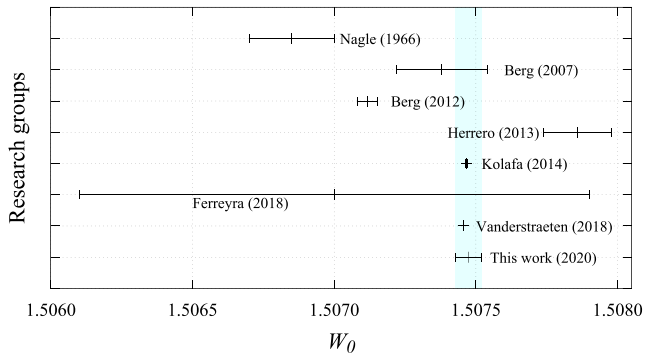


**FIG. 10**. Evaluates of $W_0$ by several research groups. The shaded area (light blue region) corresponds to the range of our final estimate.

**TABLE III**. Comparisons of the estimates by various methods.

| Group | Methods | $W_0$ | $\Delta W_0$ | $S_0$[a] | $\Delta S_0$[a] |
|---|---|---|---|---|---|
| Nagle[6] | Series expansion | 1.506 85 | 0.000 15 | 0.814 796 | 0.000 198 |
| Berg[7] | Multicanonical algorithm | 1.507 38 | 0.000 16 | 0.815 50 | 0.000 21 |
| Berg[10] | Multicanonical algorithm | 1.507 117 | 0.000 035 | 0.815 149 | 0.000 046 |
| Herrero[15] | Thermodynamic integration | 1.507 86 | 0.000 12 | 0.816 13 | 0.000 16 |
| Kolafa[16] | Thermodynamic integration | 1.507 467 4 | 0.000 003 8 | 0.815 610 3 | 0.000 0051 |
| Ferreyra[18] | Wang–Landau algorithm | 1.507 0 | 0.000 9 | 0.814 78 | 0.000 12 |
| Vanderstraeten[19] | PEPS algorithm | 1.507 456 | | 0.815 595 3 | |
| This work | REWL-MUCAREM | 1.507 472 | 0.000 047 | 0.815 615 | 0.000 063 |

[a]We used the relation $S_0 = R \ln W_0$, where $R = 1.9872$ [cal/(mol K)].

We remark that our previous evaluation[10] in 2012 by MUCA gives a value outside the error bars. However, we considered that our latest estimate is more reliable than that of the previous one because of the accuracy of the random number generator. The Metropolis criteria based on the MUCA weight factor in Eq. (14) might not have worked properly in large systems (especially, the system for $N = 2880$) in 2012.[10] Thus, we want to consider the effects of the accuracy of random numbers on MC simulations in Subsection IV B.

## B. Validity of random numbers

There is no doubt that the quality of pseudo-random number generators strongly affects the results of Monte Carlo simulations. Pseudo-random number generators have their own characteristics, for example, periodicity of random numbers. Here, we want to discuss the minimum values that can be generated by random number generators and the effects on the MUCA MC simulations.

We compared two well-known pseudo-random number generators, namely, the Marsaglia pseudo-random number generator[39] and Mersenne Twister pseudo-random number generator.[37] The Marsaglia generator was employed in our previous studies.[7,9,10] The Mersenne Twister generator was used in this work. The source codes are found in Refs. 14 and 38.

In order to compare the accuracy of random numbers, pseudo-random numbers were generated $10^{11}$ times by these generators. The generated values less than $5.0 \times 10^{-7}$ by the Marsaglia generator (green dots) and Mersenne Twister generator (purple dots) are plotted in Fig. 11. Although random numbers by the Mersenne Twister generator seem to make a uniform distribution, we can see only a discrete distribution by Marsaglia generators. The minimum random number value by the Marsaglia generator was 0 and the next minimum value was $5.9605 \times 10^{-8}$. The random number seeds were seed 1 = 11 and seed 2 = 20. It means that the Marsaglia generator we employed cannot generate the values within $(0, 5.9605 \times 10^{-8})$ as a random number. On the other hand, the minimum random number value by the Mersenne Twister generator (the random number seed was 5489) was $4.9759 \times 10^{-12}$ in our test, which is smaller than the value $5.9605 \times 10^{-8}$ by Marsaglia. We remark that the Mersenne Twister generator we employed can generate 0, although we could not observe 0 as the minimum random number value in this test run.

In the two-state model, the transition probability $w(X_0 \to X_1) = \exp(-\Delta S)$, where $\Delta S = \ln n_1 - \ln n_0$, during MUCA simulations from the ground state $X_0$ to the first excited state $X_1$ is shown in Fig. 12. The inset in Fig. 12 shows the differences of the estimate of entropy $\Delta S$ between the ground state (the value of entropy is $\ln n_0$) and the first excited state (the value of entropy is $\ln n_1$). It is clear that the difference becomes larger as the number of molecules increases. Thus, the acceptance probability around the ground state becomes small. The $w(X_0 \to X_1)$ is approximately $e^{-16}$ ($\simeq 1.125 \times 10^{-7}$) for $N = 4704$. The Marsaglia generator will not work properly because of the poor uniformity of random numbers. Hence, we may not have obtained a proper estimate for $N = 2880$ in our previous work in Ref.

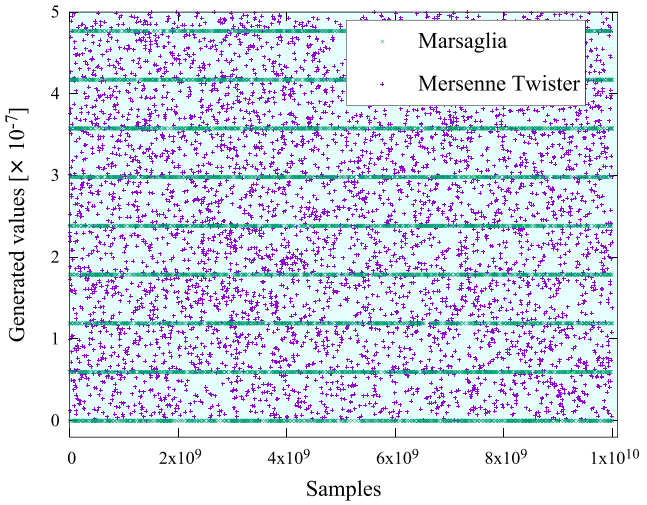


**FIG. 11**. Generated random numbers by the Marsaglia generator (green) and Mersenne Twister generator (purple). Although the purple dots seem to be distributed uniformly, green dots only take nine discrete values [0, 0.596 05, 1.192 10, 1.788 15, 2.384 20, 2.980 25, 3.576 30, 4.172 35, and 4.768 40 ($\times 10^{-7}$)].

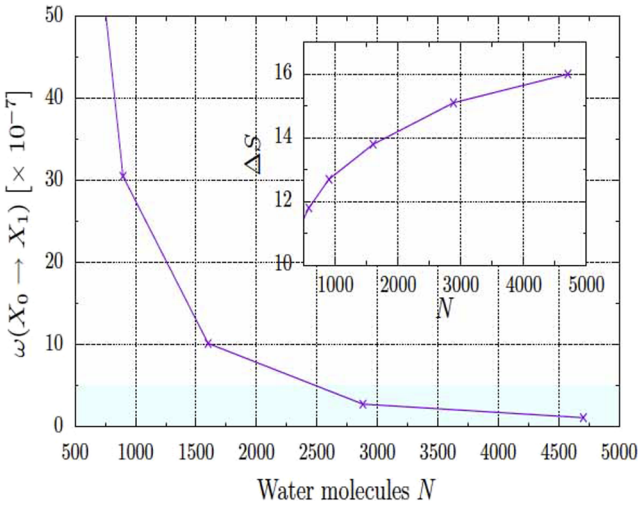


**FIG. 12**. Transition probability [$\omega(X_0 \to X_1) = \exp[-\Delta S]$] from the ground state $X_0$ (the estimated dimensionless entropy is $\ln n_0$) to the first excited states $X_1$ (the estimated dimensionless entropy is $\ln n_1$) in the two-state model. Here, $\Delta S$ is defined by $\Delta S = \ln n_1 - \ln n_0$. The inset shows $\Delta S$. The shaded area (light blue region) corresponds to the range of the ordinate in Fig. 11.

10. This is the reason why our latest estimate of the residual entropy {$S_0 = 0.815\,615 \pm 0.000\,063$ [cal/(mol K)]} in this article is different from our previous result {$S_0 = 0.815\,148 \pm 0.000\,047$ [cal/(mol K)]}. We remark that there is a sophisticated Marsaglia random number generator to alleviate the discrete problem by combining two Marsaglia random numbers into one.[14]

## V. CONCLUSIONS

Although the theoretical or experimental estimate is still difficult, the residual entropy of Ice Ih is becoming one of good models for testing the accuracy of simulation algorithms because of the rapid computational development in recent years. However, there seem to be small disagreements among the results of these simulations. The exact residual entropy of Ice Ih has yet to be obtained. In this article, we estimated the residual entropy by the REWL-MUCAREM simulations. Our final estimate of the residual entropy $S_0$ of Ice Ih is $S_0 = 0.815\,615 \pm 0.000\,063$ [cal/(mol K)]. In order to estimate the residual entropy with higher accuracy than our latest results, the calculation of $W_0$ on systems larger than $N = 4704$ will be necessary. Although our final estimate is slightly different from that of the previous MUCA simulation in Ref. 10, it agreed well with the results of several simulation groups, and three different computational groups gave almost the same estimates. We also discussed the importance of the uniformity of pseudo-random number generators.

The REWL-MUCAREM strategy can be useful to estimate the DOS with high accuracy for the systems that have rough energy landscapes, for example, spin-glass or protein systems. By combining with the reweighting techniques, detailed information about the systems can be obtained. Moreover, the REWL-MUCAREM protocol can also be used in molecular dynamics (MD) simulations. The problem of discrete random numbers in MC simulations can be avoided by MD simulations. Perhaps, *statistical temperature molecular dynamics* (STMD) *method*[40,41] or *meta-dynamics algorithm*,[42–44] which has a close relationship to WL, will be useful together with the REWL-MUCAREM. In this case, we can incorporate many such techniques that improve the efficiency of sampling (see Ref. 45) into the REWL-MUCAREM MD. We hope that the REWL-MUCAREM strategy will give us more reliable insights into complex systems.

## ACKNOWLEDGMENTS

We thank the referees for careful reading of our manuscript and for providing constructive suggestions. Some of the computations were performed on the supercomputers at the Supercomputer Center, Institute for Solid State Physics, University of Tokyo.

## DATA AVAILABILITY

The data that support the findings of this study are available within the article.

## REFERENCES

[1] W. F. Giauque and M. F. Ashley, Phys. Rev. **43**, 81 (1933).
[2] J. D. Bernal and R. H. Fowler, J. Chem. Phys. **1**, 515 (1933).
[3] L. Pauling, J. Am. Chem. Soc. **57**, 2680 (1935).
[4] See https://physics.nist.gov/cgi-bin/cuu/Value?r for Molar gas constant.
[5] L. Onsager and M. Dupuis, "The electrical properties of ice," in *Termodinamica dei Processi Irreversibili, Rendiconti della Scuola Internazionale di Fisica "Enrico Fermi," Corso X, Varenna, 1959* (Nicola Zanichelli, Bologna, 1960), pp. 294–315.
[6] J. F. Nagle, J. Math. Phys. **7**, 1484 (1966).
[7] B. A. Berg, C. Muguruma, and Y. Okamoto, Phys. Rev. B **75**, 092202 (2007).
[8] B. A. Berg and W. Yang, J. Chem. Phys. **127**, 224502 (2007).
[9] C. Muguruma, Y. Okamoto, and B. A. Berg, Phys. Rev. E **78**, 041113 (2008).
[10] B. A. Berg, C. Muguruma, and Y. Okamoto, Mol. Simul. **38**, 856 (2012).
[11] B. A. Berg and T. Neuhaus, Phys. Lett. B **267**, 249 (1991).
[12] B. A. Berg and T. Neuhaus, Phys. Rev. Lett. **68**, 9 (1992).
[13] W. Janke, Physica A **254**, 164 (1998).
[14] B. A. Berg, *Markov Chain Monte Carlo Simulations and Their Statistical Analysis: With Web-Based Fortran Code* (World Scientific, Singapore, 2004).
[15] C. P. Herrero and R. Ramírez, Chem. Phys. Lett. **568-569**, 70 (2013).
[16] J. Kolafa, J. Chem. Phys. **140**, 204507 (2014).
[17] M. V. Ferreyra, G. Giordano, R. A. Borzi, J. J. Betouras, and S. A. Grigera, Eur. Phys. J. B **89**, 51 (2016).
[18] M. V. Ferreyra and S. A. Grigera, Phys. Rev. E **98**, 042146 (2018).
[19] L. Vanderstraeten, B. Vanhecke, and F. Verstraete, Phys. Rev. E **98**, 042145 (2018).
[20] T. Vogel, Y. W. Li, T. Wüst, and D. P. Landau, Phys. Rev. Lett. **110**, 210603 (2013).
[21] T. Vogel, Y. W. Li, T. Wüst, and D. P. Landau, Phys. Rev. E **90**, 023302 (2014).
[22] Y. Sugita and Y. Okamoto, Chem. Phys. Lett. **329**, 261 (2000).
[23] A. Mitsutake, Y. Sugita, and Y. Okamoto, J. Chem. Phys. **118**, 6664 (2003).
[24] A. Mitsutake, Y. Sugita, and Y. Okamoto, J. Chem. Phys. **118**, 6676 (2003).
[25] T. Hayashi and Y. Okamoto, Phys. Rev. E **100**, 043304 (2019).
[26] R. R. P. Singh and J. Oitmaa, Phys. Rev. B **85**, 144414 (2012).
[27] B. A. Berg and T. Celik, Phys. Rev. Lett. **69**, 2292 (1992).
[28] A. M. Ferrenberg and R. H. Swendsen, Phys. Rev. Lett. **61**, 2635 (1988).
[29] F. Wang and D. P. Landau, Phys. Rev. Lett. **86**, 2050 (2001).

[30]F. Wang and D. P. Landau, Phys. Rev. E **64**, 056101 (2001).
[31]K. Hukushima and K. Nemoto, J. Phys. Soc. Jpn. **65**, 1604 (1996).
[32]Y. Sugita and Y. Okamoto, Chem. Phys. Lett. **314**, 141 (1999).
[33]R. H. Swendsen and J.-S. Wang, Phys. Rev. Lett. **57**, 2607 (1986).
[34]E. Marinari, G. Parisi, and J. Ruiz-Lorenzo, "Numerical simulations of spin glass systems," in *Spin Glasses and Random Fields*, edited by A. P. Young (World Scientific, Singapore, 1997), pp. 59–98.
[35]A. M. Ferrenberg and R. H. Swendsen, Phys. Rev. Lett. **63**, 1195 (1989).
[36]S. Kumar, J. M. Rosenberg, D. Bouzida, R. H. Swendsen, and P. A. Kollman, J. Comput. Chem. **13**, 1011 (1992).
[37]M. Matsumoto and T. Nishimura, ACM Trans. Model. Comput. Simul. **8**, 3 (1998).
[38]See http://www.math.sci.hiroshima-u.ac.jp/m-mat/MT/VERSIONS/FORTRAN/mt19937-64.f95 for Mersenne Twister Random Number Generator for Fortran.
[39]G. Marsaglia, A. Zaman, and W. Wan Tsang, Stat. Probab. Lett. **9**, 35 (1990).
[40]J. Kim, J. E. Straub, and T. Keyes, Phys. Rev. Lett. **97**, 050601 (2006).
[41]J. Kim, J. E. Straub, and T. Keyes, J. Phys. Chem. B **116**, 8646 (2012).
[42]A. Laio and M. Parrinello, Proc. Natl. Acad. Sci. U. S. A. **99**, 12562 (2002).
[43]T. Huber, A. E. Torda, and W. F. van Gunsteren, J. Comput.-Aided Mol. Des. **8**, 695 (1994).
[44]H. Grubmüller, Phys. Rev. E **52**, 2893 (1995).
[45]C. Junghans, D. Perez, and T. Vogel, J. Chem. Theory Comput. **10**, 1843 (2014).